ACS APPLIED MATERIALS & INTERFACES

Research Article

www.acsami.org

Composite Films of Oxidized Multiwall Carbon Nanotube and Poly(3,4-ethylenedioxythiophene): Polystyrene Sulfonate (PEDOT:PSS) As a Contact Electrode for Transistor and Inverter Devices

Dong-Jin Yun and Shi-Woo Rhee*

System on Chip Chemical Process Research Center, Department of Chemical Engineering, Pohang University of Science and Technology (POSTECH), Pohang 790-784, Korea

ABSTRACT: Composite films of multiwall carbon nanotube (MWNT)/poly(3,4-ethylenedioxythiophene) polymerized with poly(4-styrenesulfonate) (PEDOT:PSS) were prepared by spin-coating a mixture solution. The effect of the MWNT loading and the MWNT oxidation, with acid solution or ultraviolet (UV)-ozone treatment, on the film properties such as surface roughness, work function, surface energy, optical transparency and conductivity were studied. Also pentacene thin film transistors and inverters were made with these composite films as a contact metal and the device characteristics were measured. The oxidation of MWNT reduced the conductivity of MWNT/PEDOT:PSS composite film but increased the work function and transparency. UV-ozone treated MWNT/PEDOT:PSS composite film showed higher conductivity (14000 Ω/□) and work function (4.9 eV) than acid-oxidized MWNT/PEDOT:PSS composite film and showed better performance as a source/drain electrode in organic thin film transistor (OTFT) than other types of MWNT/PEDOT:PSS composite films. Hole injection barrier of the UV-ozone treated MWNT/PEDOT:PSS composite film with pentacene was significantly lower than any other films because of the higher work function.

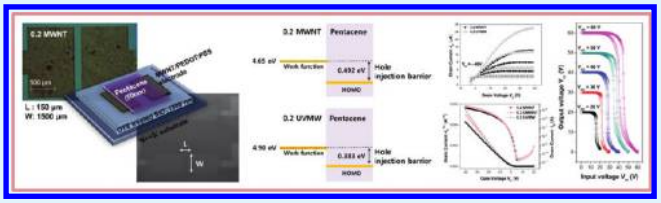

KEYWORDS: *multiwalled carbon nanotube, CNT:PEDOT composite, oxidized CNT, organic thin film transistor, work function, hole injection barrier*

1. INTRODUCTION

Many groups have studied electrode materials for electronic devices including organic thin film transistor (OTFT), organic photovoltaic (OPV), dye-sensitized solar cell (DSSC) and organic light-emitting diode (OLED) to improve the device performance with low-cost materials and processes.[1−4] Carbon nanotube (CNT) is an attractive candidate for this application due to its high conductivity, stability and optical transmittance.[3,5−8] CNT material has been applied in various fields including OLED, OTFT, OPV, and DSSC as an emitting, catalytic, or transparent electrodes.[9−12] However, CNT has an intrinsic problem because it is difficult to disperse uniformly in most solvents, and many groups have tried to solve this problem for decades.[13,14] The oxidation of CNT and grafting of polymer onto CNT are the most widely utilized methods to improve the dispersion of CNT in solvents.[13−16] The polymer grafting onto CNT can improve the solubility of CNT in a polar solvent and conductivity of CNT film can be further improved in combination with highly conductive polymer.[17,18] Among them, poly (3,4-ethylenedioxythiophene) polymerized with poly (4-styrenesulfonate) (PEDOT: PSS) is a good candidate with a high conductivity (0.1 to 1 × 10^3 S/cm) and a good solubility in polar solvents.[19−21] On the basis of these advantages, studies on the application of CNT, PEDOT:PSS, or CNT/PEDOT:PSS composite films as an electrode material have been reported in recent years and it was reported that the film properties including work function, morphology and sheet resistance were influenced by the MWNT/PEDOT:PSS composition.[22] Despite the high conductivity, work function of multiwall carbon nanotube (MWNT)/PEDOT:PSS films (∼ 4.7 eV) is not high enough as a source and drain (S/D) electrode in p-type OTFT.[22]The oxidation of CNT using acid solution (HCl or HNO_3) would increase the work function along with better dispersion in polar solvents owing to the introduction of −OH, −COO−, or −COOH functional groups, but acid-solution treated CNT shows much poorer conductivity than as-purchased CNT due to the ring-opening or breaking of CNT chains.[16−18] On the other hand, the oxidation of CNT using ultraviolet(UV)-ozone treatment was recently reported and using this method, dispersion of CNT was improved with only slight conductivity reduction because functional groups were formed on the surface of the CNT chain without much chain breaking during UV treatment.[23,24]

So far, the effect of CNT oxidation on the film properties of CNT/PEDOT:PSS composites has not been studied and in this work, as purchased MWNT was oxidized with acid solution or UV-ozone treatment and MWNT/PEDOT:PSS composite solutions were prepared with various compositions. The MWNT/PEDOT:PSS composite films were prepared with spin-coating on SiO_2 (300 nm) surface thermally grown on Si substrate and the film properties such as resistivity, work function, morphology, and surface energy were measured. The pentacene-OTFTs

Received: November 20, 2011
Accepted: January 20, 2012
Published: January 20, 2012

and complementary inverters with MWNT/PEDOT:PSS composite films as a source/drain (S/D) electrode were fabricated and their performances were evaluated.

2. EXPERIMENTAL SECTION

PEDOT:PSS solution (CLEVIOS PH500: 1 wt % in water) and MWNT were purchased from H.C. Starck and Carbon Nanomaterial Technology Co., respectively. As-purchased MWNT chains were examined by high-resolution TEM measurement (JEM-2200FS, JEOL) to observe shape, length and wall number. To prepare oxidized MWNT in acid solution (Oxy MWNT), we refluxed as-purchased MWNT in a mixture of sulfuric and nitric acid (volume ratio of 3:1) at ~100 °C for 1 h and the mixture was filtered using polycarbonate membrane of 0.2 μm pore size and dried in a vacuum oven at ~60 °C for 24 h. UV-ozone treated MWNT (UV MWNT) was prepared with UV (wavelength: ~254 nm)-ozone treatment using high intensity mercury lamp in UV-tip cleaner (UV/Ozone Procleaner, BiOFORCE) for 6 h. To prevent the gel formation due to the entanglement and aggregation between MWNT and PEDOT:PSS, we diluted 10 mL of the as-purchased PEDOT:PSS solution with equal volume of deionized water before we added 0.2 g as-purchased MWNT (0.2 MWNT). After 30 min ultrasonication process, MWNT was well-dispersed and the MWNT/PEDOT:PSS solution remained stable without any sediment for more than a week. The dispersion of oxidized MWNT in PEDOT:PSS solution could be improved because of the functionalization of the surface during the oxidation process and MWNT/PEDOT:PSS solution were prepared by adding 0.2 or 0.3 g of Oxy or UV MWNT into 20 mL of the as-purchased PEDOT:PSS solution without the dilution process (0.2, 0.3 OMWNT or UVMW). MWNT/PEDOT:PSS composite films were prepared using spin-coating (5000 rpm) of the MWNT/PEDOT:PSS solution on SiO_2 (300 nm)/N++Si substrate (Silicon Material Inc.) and then annealed in vacuum oven at ~100 °C for 2 h. The schematic diagram of the film forming process is shown in Figure 1a.

The pentacene TFTs with MWNT/PEDOT:PSS S/D electrodes were fabricated and their performance was characterized. OTS (octadecyltrichlorosilane) monolayer was formed on the oxide surface to improve the interface property of pentacene on insulator. Prior to the formation of OTS monolayer, SiO_2 (300 nm)/N++Si substrate was dipped in piranha solution (H_2SO_4: H_2O_2 = 7:4 vol%) for 1 h at ~100 °C and cleaned in UV tip cleaner for 30 min. Then, the substrate was dipped in the 1 mM OTS-toluene (purchased from Aldrich Chemical Co.) solution for 2 h at the low temperature of ~4 °C and washed out in toluene and acetone for 30 min each with ultrasonication. Finally, OTS-treated substrate was annealed in a vacuum chamber for 2 h at 150 °C and kept in vacuum chamber at 50 °C.

Lift-off process was used to pattern the S/D electrode of the pentacene OTFT. Photoresist (negative type PR, AZ5214-E) was spin-coated on the substrate with a speed of 5000 rpm for 45 s and the layer was exposed to UV light of ~350 nm major wavelength through the mask and then washed out with developer and DI water. Subsequently, the substrate was exposed to UV-ozone in a UV tip cleaner for 10 min and MWNT/PEDOT:PSS film for S/D electrode was spin-coated (5000 rpm) on the whole substrate surface. Then the substrate was annealed in a vacuum oven at ~100 °C for 2 h and washed in acetone with ultrasonication. The patterning process of the MWNT/PEDOT:PSS film to be used as a S/D electrode in OTFT was briefly summarized elsewhere.[22] Pentacene films as an organic semiconductor in OTFTs were deposited at 70 °C with a deposition rate of 0.2–0.3 Å/s in an organic molecular beam deposition (OMBD) system at a pressure of 2×10^{-6} Torr. This fabrication procedure was also utilized to prepare a p-type part of an inverter (channel length: 100 μm and channel width: 1000 μm) and n-type organic semiconductor (N, N′-ditridecyl perylene diimide (PTCDI-C13)) films were deposited at room temperature with a rate of 0.2–0.3 Å/s in an OMBD system.

Sheet resistance of the MWNT/PEDOT:PSS film was measured with 4-point probe method (KEITHLEY 2400 source meter) and the top-view of the S/D electrodes patterned using photolithography were observed with optical microscope (OM). The morphology of the MWNT/PEDOT:PSS film was investigated using atomic force measurement (AFM, Veeco Nanoscope V in NCNT) and secondary emission microscope (SEM, JEOL JSM-7401F). The bonding state and work function of the MWNT/PEDOT:PSS film were investigated with X-ray photoemission spectroscopy (XPS) and ultraviolet photoemission spectroscopy (UPS) measurement. The current–voltage (I–V) characteristics of the pentacene TFT and inverter were measured at room temperature using Agilent E5270A precision semiconductor parameter analyzer and Keithley 4200 semiconductor characterization system.

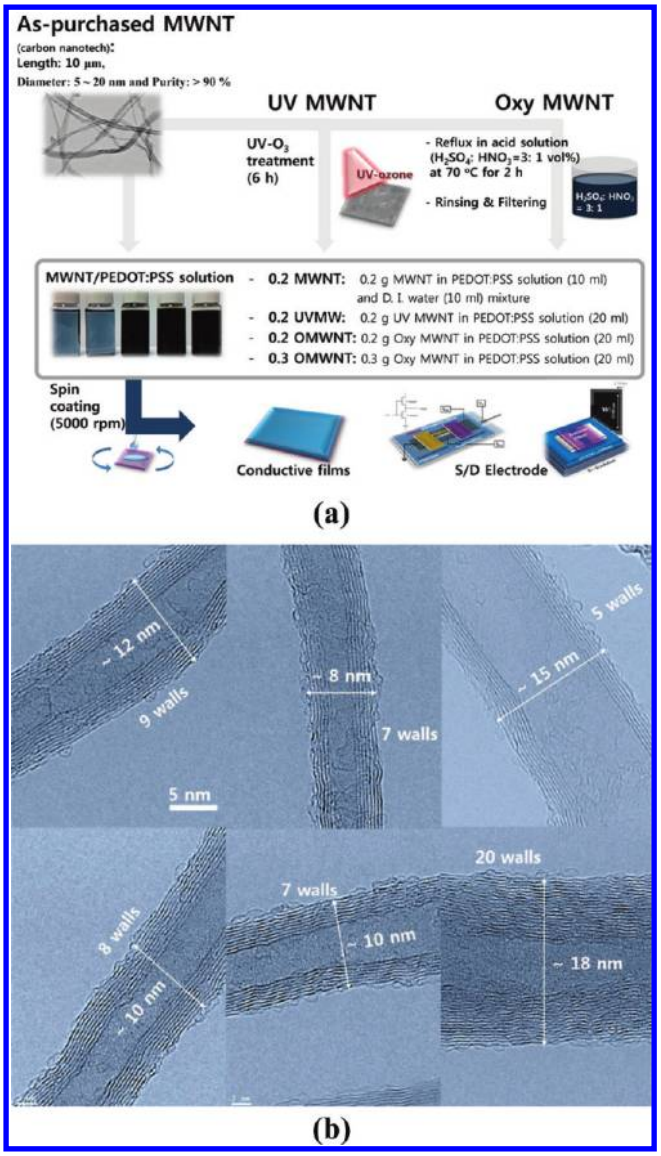

Figure 1. (a) Schematic diagram showing how to prepare various types of MWNT/PEDOT:PSS films and (b) TEM images of the as-purchased MWNTs, which have different wall number and diameter.

3. RESULTS AND DISCUSSION

Figure 1b shows TEM images of as-purchased MWNTs, which have different wall number and diameter. MWNTs showed multi walls between 5 and 20 wall number and diameter also varied (5–20 nm) depending on the wall number. Several impurities around the MWNT chains were also observed and they were mainly originated from the metal catalyst. As described in the experimental section and Figure 1a, various MWNT/PEDOT:PSS solutions were prepared with as-purchased MWNT, UV MWNT, or Oxy MWNT and PEDOT:PSS solution, 0.2 MWNT (films made with MWNT 0.985 wt % in solution and MWNT/PEDOT:PSS = 2:1 weight ratio), 0.2 UVMW (UV-treated MWNT 0.98 wt % in solution

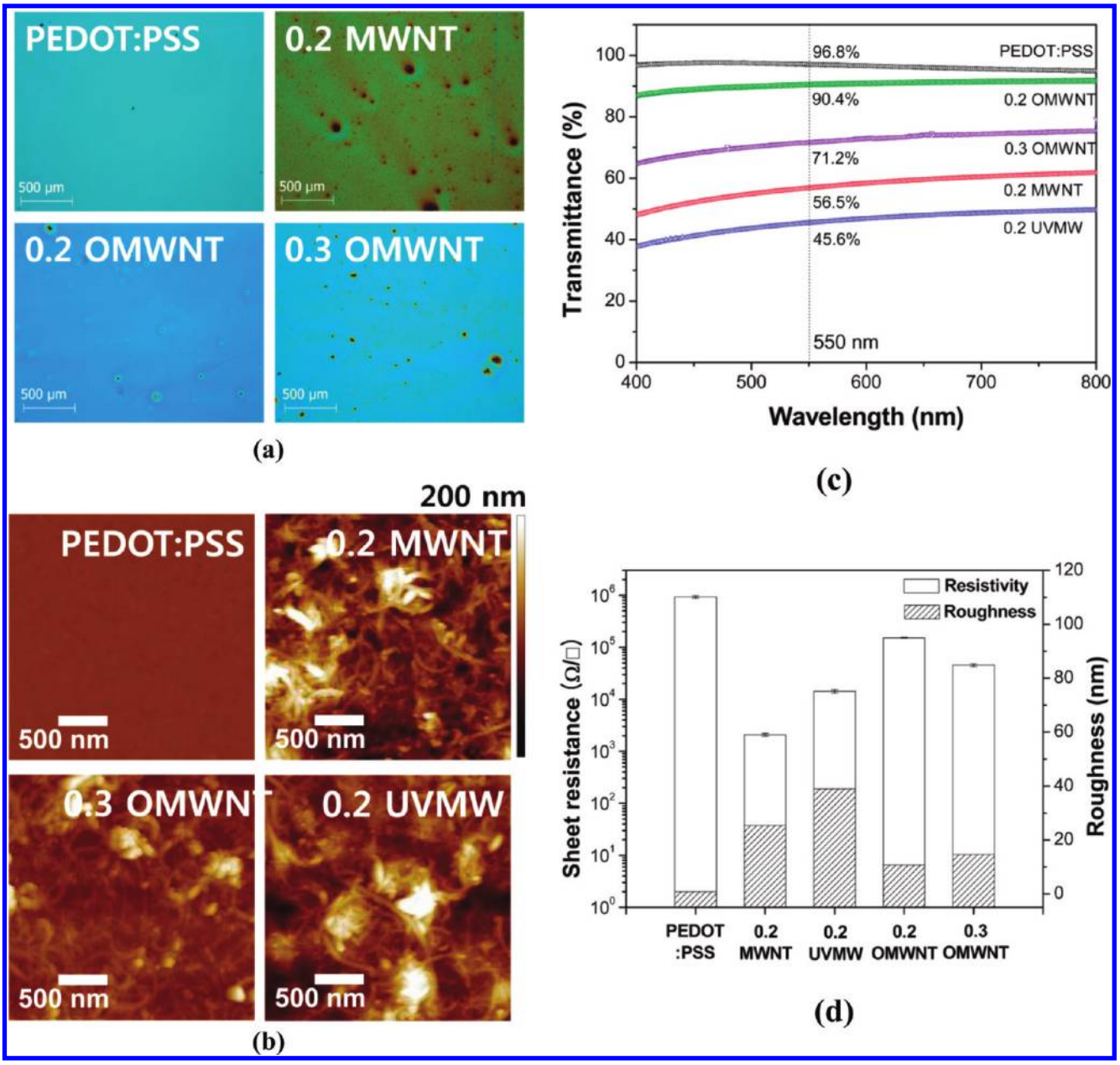

Figure 2. Morphology of MWNT/PEDOT:PSS films observed with (a) OM and (b) AFM; (c) transmittance of various MWNT/PEDOT:PSS films in the visible region (400−800 nm wavelength); and (d) roughness and sheet resistances of various MWNT/PEDOT:PSS films.

and UV MWNT/PEDOT:PSS = 1:1 weight ratio), 0.2 OMWNT (Oxy MWNT 0.98 wt % in solution and Oxy MWNT/PEDOT:PSS = 1:1 weight ratio) and 0.3 OMWNT (Oxy MWNT 1.46 wt % in solution and Oxy MWNT/PEDOT:PSS = 3:2 weight ratio) films were prepared on SiO_2 (300 nm)/Si substrates. The properties such as morphology, resistivity and work function were highly dependent on the MWNT oxidation state as well as the MWNT concentration in PEDOT:PSS solution. The morphology of the spin-coated MWNT/PEDOT:PSS film was investigated using OM and AFM images as shown in panels a and b in Figure 2. PEDOT:PSS film shows smooth surface morphology without any agglomeration, but the MWNT aggregation was observed in the MWNT/PEDOT:PSS composite film from the entanglement of the MWNT chains. In spite of the higher MWNT and PEDOT:PSS concentration in the solution, the number and size of MWNT agglomerations in the 0.3 OMWNT (or 0.2 OMWNT) film was smaller than 0.2 MWNT because the CNT dispersion was improved by the formation of the functional group and the ring-opening or chain break in the CNT during the oxidation process.[16−18,25] The transmittance at visible region (400−800 nm wavelength) of various MWNT/PEDOT:PSS films were compared as shown in Figure 2c. OMWNT films on the glass substrate showed high transparency (0.2 OMWNT: 90.4% and 0.3 OMWNT: 71.2% at 550 nm), which is comparable to PEDOT:PSS film, but 0.2 UVMW and 0.2 MWNT films on the glass substrate were semitransparent at visible region (0.2 UVMW: 45.6% and 0.2 MWNT: 56.5% at 550 nm) because of the dense tangles of MWNT long chains. MWNT chains were not broken after UV treatment and therefore, the configuration of CNT chains in 0.2 UVMW is almost the same as 0.2 MWNT. Even though the UV treatment has an effect on the transparency of the composite film, 0.2 UVMW actually showed lower transparency compared with 0.2 MWNT, in spite of the MWNT functionalization. We believe

Table 1. Film Properties of the CNT/PEDOT:PSS Film and the Characteristics of the Pentacene TFT with Various Types of CNT/PEDOT:PSS S/D Electrode

	MWNT/PEDOT:PSS film properties						characteristics of OTFTs		
materials (MWNT wt % in PEDOT:PSS solution)	wt% ratio between MWNT and PEDOT:PSS	thickness (nm)	sheet resistivity (Ω/□)	roughness (nm)	optical transmit-ttance at 550 nm (%)	work function (Φ)	field-effect Mobility ($cm^2/(V\ s)$)	on/off current ratio	threshold voltage (V_{th})
PEDOT:PSS[22] (0.985 w(0.985 wt %)t %)		50	980000 ± 230000	0.815	96.8	4.95	0.05 ± 0.05	~1×10^5	1.45 ± 0.2
0.2 MWNT (0.980 wt %)	2:1	150 ± 50	2150 ± 500	25.4	56.5	4.70	0.24 ± 0.01	~5×10^5	−4.4 ± 0.5
0.2 OMWNT (0.980 wt %)	1:1	100 ± 20	156000 ± 10000	10.7	90.4				
0.3 OMWNT (1.46 wt %)	3:2	120 ± 20	46800 ± 3000	14.6	71.2	5.09	0.35 ± 0.01	~5×10^5	−4.2 ± 0.5
0.2 UVMW (0.980 wt %)	1:1	150 ± 50	14000 ± 2000	39	45.6	4.90	0.37 ± 0.01	~5×10^5	−3.8 ± 0.5

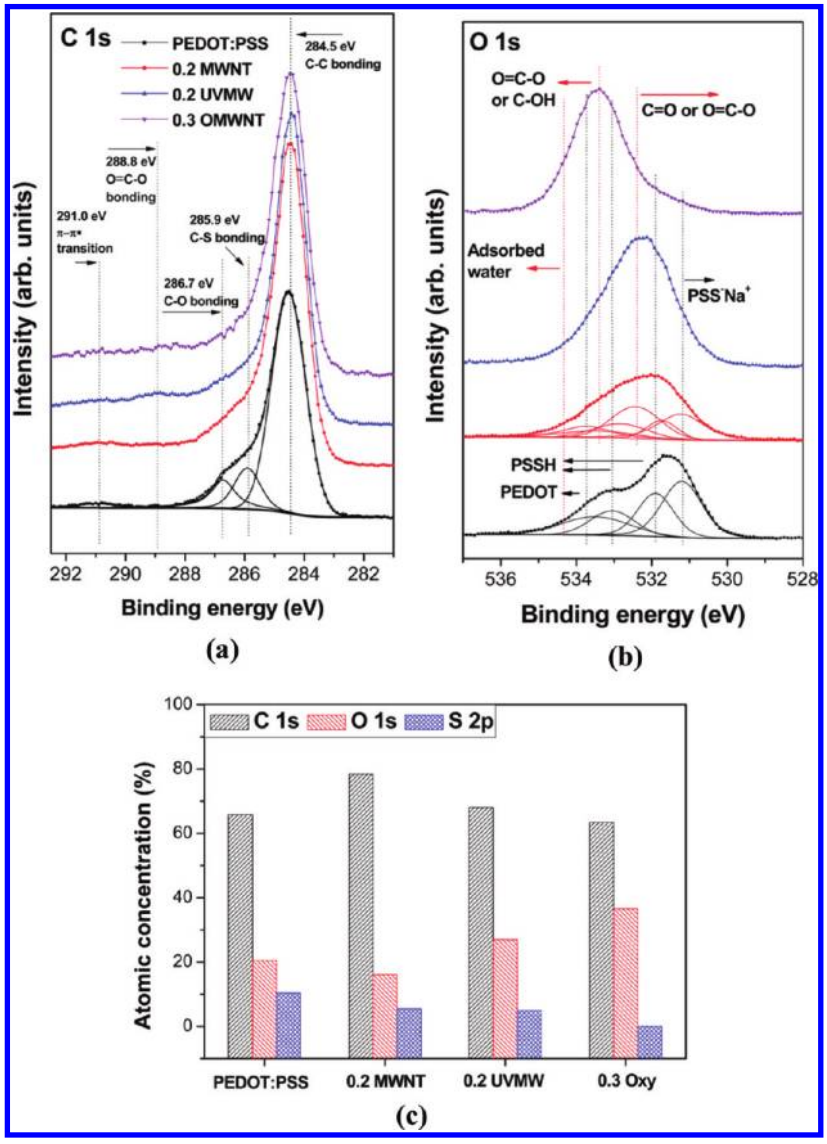

Figure 3. Comparative XPS spectra of (a) C 1s and (b) O 1 s core levels and (c) the atomic composition at the surface region of various MWNT/PEDOT:PSS films.

that low transparency of 0.2 UVMW results from the higher concentration of PEDOT:PSS in the solution. As summarized in table 1, the PEDOT:PSS concentration in 0.2 UVMW solution is twice higher than that of 0.2 MWNT solution, and therefore UV MWNT chains in 0.2 UVMW are more densely packed and covered with PEDOT:PSS molecules. Roughness (calculated from AFM images of 2.5 × 2.5 μm^2) of 0.2 UVMW was comparable with 0.2 MWNT, as shown in Figure 2d. Apart from morphology, 0.2 UVMW showed distinct electrical properties (work function and sheet resistance) and the sheet resistance of 0.2 UVMW or 0.3 OMWNT is much lower than that of PEDOT:PSS film but higher than that of 0.2 MWNT. This result confirmed that the electrical properties of MWNT/PEDOT:PSS films were highly dependent on the oxidation process of MWNT.

Panels a and b in Figure 3 show comparative XPS spectra of C 1s and O 1s core levels at the surface regions of various MWNT/PEDOT:PSS films. PEDOT:PSS has chemical bonding among carbon, sulfur, oxygen, and hydrogen atoms and MWNT is

dx.doi.org/10.1021/am201622j | ACS Appl. Mater. Interfaces 2012, 4, 982–989

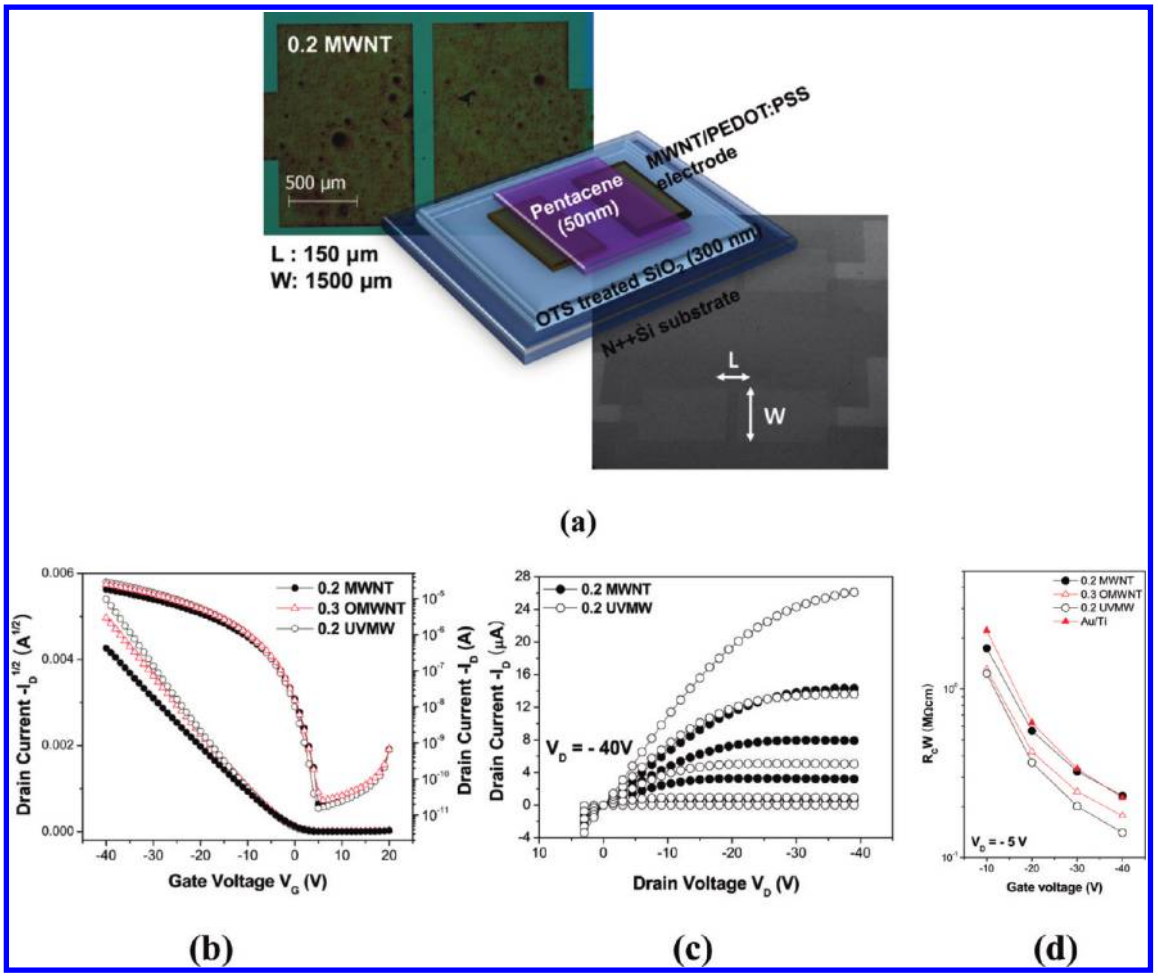

Figure 4. (a) Schematic of bottom-contact pentacene TFTs with MWNT/PEDOT:PSS S/D electrodes, (b) the transfer and (c) output characteristics of the pentacene TFTs with various MWNT/PEDOT:PSS S/D electrodes, and (d) the contact resistance between MWNT/PEDOT:PSS electrode and pentacene.

composed of the carbon−carbon bonding. The main asymmetric peak at 284.5 eV was assigned to the sp^3 and sp^2 carbon−carbon bonding and the tail peaks at 285.9 and at 286.8 eV were assigned to the carbon−sulfur and carbon−oxygen bonding. The small peak at 291.0 eV indicating $\pi-\pi^*$ transition in PEDOT:PSS film was also observed as shown in Figure 3a.[19,26,27] The intensity of the main peak at 284.5 eV (C 1s core level) in MWNT/PEDOT:PSS film was increased compared with the PEDOT:PSS film without a change in the position but there is no significant variation in the XPS spectrum due to the oxidation of MWNT. The O 1s core levels of PEDOT:PSS consists of the peaks from PSSH, PSS^-Na^+ and PEDOT but in the MWNT/PEDOT:PSS film, the intensities were decreased without change in the peak position just like S in the film. Small peaks indicating −COH, −COO, −COOH, and physically absorbed O atoms newly appeared at 0.2 MWNT.[28,29] O 1s core levels of 0.2 UVMW and 0.3 OMWNT were composed of various oxidation states of MWNT as well as PEDOT:PSS and among them, the −COOH and −COH bonding states became main peaks of O 1s core levels in the 0.3 OMWNT film. The atomic concentration of carbon in the 0.2 MWNT film was higher than PEDOT:PSS film and the atomic concentration of hydrogen and sulfur were slightly lower due to the MWNT chains consisting of sp^2 carbon bonding. Both 0.2 UVMW and 0.3 OMWNT films showed higher atomic concentration of oxygen component compared with 0.2 MWNT due to −COH, −COO, or −COOH group of oxidized MWNT. 0.3 OMWNT with highly oxidized MWNT showed more oxygen concentration and higher oxidation states than other films, as shown in Figure 3c.

To analyze the effect of MWNT oxidation state on the performance of the MWNT/PEDOT:PSS film as S/D electrodes, we fabricated the bottom-contact pentacene TFTs with MWNT/PEDOT:PSS S/D electrodes as shown in Figure 4a and electrical properties of them were characterized. The field-effect mobility in the saturated regime (V_D = −40 V) was calculated from the transfer curve shown in Figure 4b. Compared with the pentacene TFT with 0.2 MWNT S/D electrode (μ = 0.24 cm^2/(V s)), the pentacene TFTs with 0.2 OMWNT and 0.3 UVMW films showed higher field-effect mobilities of 0.32 and 0.39 cm^2/(V s), respectively. Output curves of the pentacene TFTs with 0.2 MWNT and 0.2 UVMW S/D electrodes were compared in Figure 4c and the pentacene TFT with 0.2 UVMW S/D electrode showed much higher drain current at the same drain voltage compared with that of 0.2 MWNT. The threshold voltage of pentacene TFTs with 0.2 UVMW and 0.3 OMWNT S/D electrodes were smaller (about −2.5 V) compared to the TFTs with 0.2 MWNT S/D electrode (V_T = −4.4 V). The contact resistance between S/D electrode and pentacene was measured by controlling the gate voltage in the range of −10 to −40 V in the linear region with the drain voltage of −5 V. As shown in Figure 4d, contact resistance values were highly dependent on the S/D electrode material and interface between 0.2 UVMW (or 0.3 OMWNT) and pentacene showed lower

dx.doi.org/10.1021/am201622j | ACS Appl. Mater. Interfaces 2012, 4, 982−989

contact resistance than the 0.2 MWNT (or Au/Ti) and pentacene. We believe that the better performance of the pentacene TFTs with 0.2 UVMW or 0.3 OMWNT is fundamentally attributable to the lower contact resistance from the higher work function of the S/D electrode.

Figure 5a shows the comparative UPS spectra of various MWNT/PEDOT:PSS films. The secondary cutoff region (E_{cutoff}) and Fermi energy (E_F) were clearly defined and the work function of the MWNT/PEDOT:PSS film was calculated using the following eq 1[1,22]

$$\varphi = h\nu\ (=21.2\ \text{eV}) - E_{\text{cutoff}} + E_{\text{Fermi}} \quad (1)$$

.Here, $h\nu$ (21.2 eV) is the incoming photon energy from He I source and the −5 V bias was applied to make a clear boundary in the E_{cutoff} region. The work function of the conductive film highly depends on the surface properties as well as bulk properties. As seen in the morphological images of 0.2 UVMW or 0.2 MWNT, MWNT chains were densely tangled at the surface region and therefore, it is believed that the surface properties including the work function highly depend on the properties of MWNT as well as those of PEDOT:PSS. The work function of PEDOT:PSS and 0.2 MWNT were measured to be 4.95 and 4.70 eV, respectively. At the surface region of 0.2 MWNT, MWNT, which has a relatively lower work function (4.6 eV) compared with that of PEDOT:PSS (5.0 eV), is densely packed and highly influences surface properties. Thus the work function of 0.2 MWNT film is almost similar with that of MWNT material. On the other hand, as the oxidation state of MWNT varies, the surface properties of MWNT/PEDOT:PSS film were highly influenced by the chain-breaking or ring-opening of MWNT during the oxidation process. As a result of this, conductivity of MWNT highly decreases but work function slightly increases owing to the addition of electron withdrawing groups such as −COH, −COO, and −COOH. 0.2 UVMW showed a high work function of 4.9 eV and the work function of 0.3 OMWNT was larger than the PEDOT:PSS film, as shown in the comparative UPS spectra of Figure 5a. The work function difference between 0.2 UVMW and 0.3 OMWNT was induced by the oxidation state of oxidized MWNT, and the differences in oxidation states of them were confirmed with XPS measurement of Figure 3b.

In p-type TFT, high work function of S/D electrode enables electrode/semiconductor interface to form low hole injection barrier and the hole loss at the interface can be minimized. The hole injection barrier is given as

$$\varphi_B = E_{\text{Homo(organic)}} - \varphi \quad (2)$$

,and here, $E_{HOMO\ (organic)}$ is the highest occupied molecular level (HOMO) of pentacene and φ is the work function of the metal as given in eq 1. The work function of the S/D electrode is a crucial factor determining the contact resistance between S/D electrode and pentacene in pentacene TFTs and the S/D electrode of high work function close to the HOMO level of pentacene can form an ohmic contact with low hole-injection barrier.[1,22,30,31]With the pentacene deposition, $E_{HOMO(organic)}$ and the shift of $E_{cutoff(metal)}$ were observed when the pentacene layer thickness was high enough and the actual hole injection barrier between the S/D electrode and pentacene can be obtained from the UPS spectra shown in panels b and c in Figure 5.[30,31] On the basis of the valence band structure of pentacene thin layers on 0.2 MWNT and 0.2 UVMW, actual hole injection barriers were calculated as shown in Figure 5d. The hole injection barrier between pentacene and 0.2 UVMW S/D electrode was 0.383 eV and this value was significantly lower than that between pentacene and 0.2 MWNT S/D electrode because of the high work function of 0.2 UVMW.

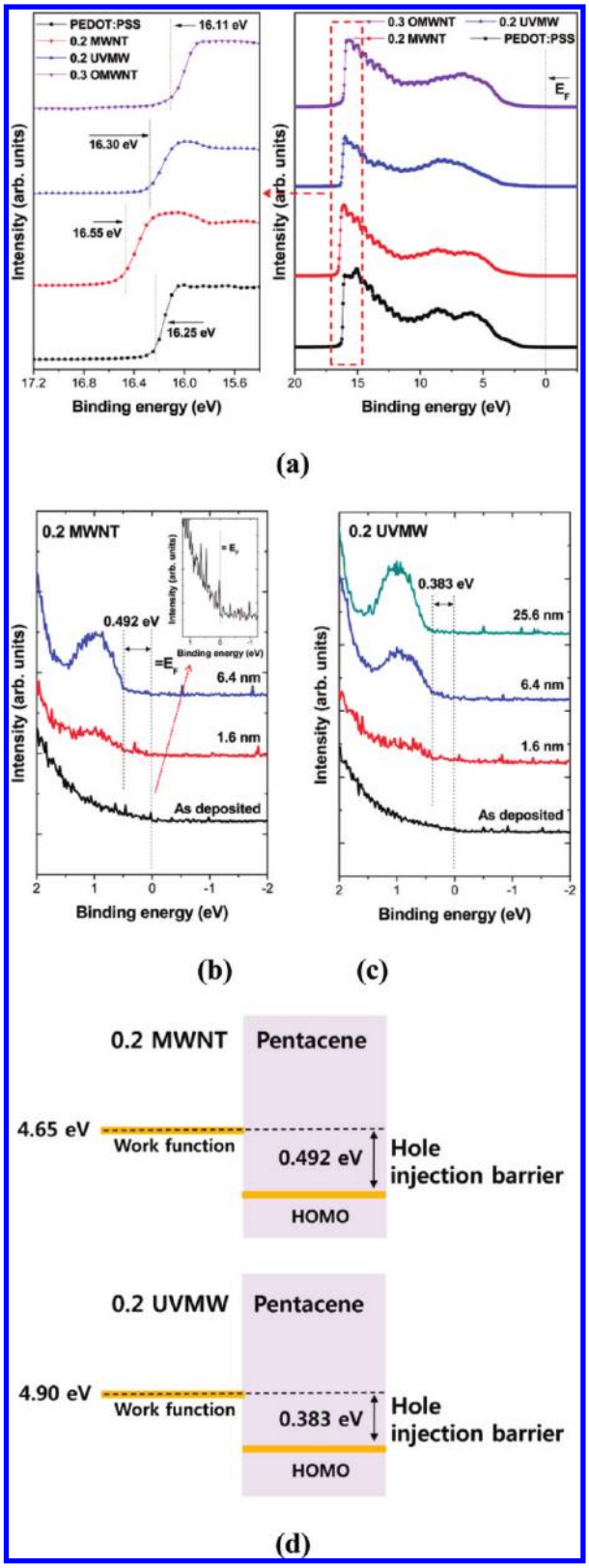

Figure 5. (a) Comparative UPS spectra including secondary cutoff and Fermi edge regions of various MWNT/PEDOT:PSS films, (b, c) UPS spectra of the pentacene layers grown on (b) 0.2 MWNT and (c) 0.2 UVMW films, and (d) the hole injection barrier between the MWNT/PEDOT:PSS film and pentacene calculated from the UPS spectra.

dx.doi.org/10.1021/am201622j | ACS Appl. Mater. Interfaces 2012, 4, 982−989

Additionally, the complementary inverter with 0.2 UVMW film as a S/D electrode was also fabricated as shown in Figure 6a and performance was compared with 0.2 MWNT S/D electrode. As compared in Figure 6d, the difference in the saturation current and mobility between p-type and n-type TFT result in the positive shift of the inverter threshold voltage. Nevertheless, the complementary inverters showed good output voltage (V_{out})−input voltage (V_{in}) characteristics as shown in Figure 6b. The V_{out} stayed close to V_{DD} at low V_{in} and abruptly dropped to 0 V above the specific V_{in}.[32,33] This behavior was from the complementary turning on and off operation of p-type (pentacene) and n-type (PTCDI-C13) TFTs. The DC gains (dV_{out}/dV_{in}) as a function of V_{in} was plotted in Figure 6c and their values were almost 50, which is much higher than DC gains (near 30) of the inverter with 0.2 MWNT S/D electrode.

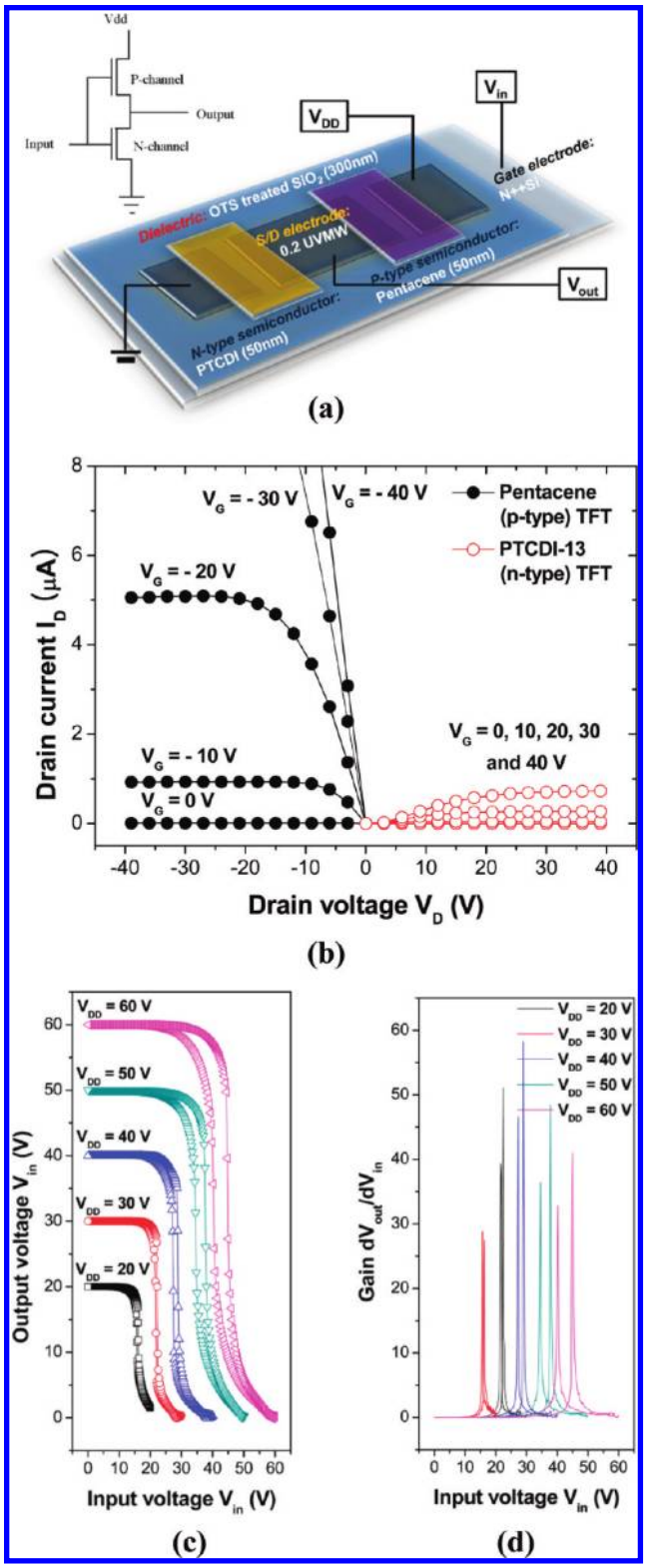

Figure 6. (a) Schematic structure of the complementary inverter with 0.2 UVMW S/D electrode, (b) comparative output characteristics of p- and n-type TFTs, (c) voltage transfer characteristics, and (d) DC gain with various V_{DD} values.

4. CONCLUSION

The effect of the MWNT oxidation on the MWNT/PEDOT:PSS composite film properties such as surface roughness, work function, surface energy, optical transparency, and conductivity were characterized. The oxidation process of MWNT reduced the conductivity of MWNT/PEDOT:PSS composite film but increased the work function due to the formation of the functional groups from the ring-opening or chain break of MWNT during oxidation process. 0.2 UVMW film showed a high work function and conductivity and exhibited excellent performance as a S/D electrode in the pentacene TFT and the complementary inverter.

AUTHOR INFORMATION

Corresponding Author

*E-mail: srhee@postech.ac.kr. Tel: 82-54-279-2265. Fax: 82-54-279-8619.

Notes

The authors declare no competing financial interest.

ACKNOWLEDGMENTS

This research was supported by the Korea Science and Engineering Foundation (KOSEF) and the Pohang Accelerator Laboratory provided the synchrotron radiation source at the 4B1 beamline was used in this study. The author D. J. Yun is grateful to Y. K. Lee and J. W. Seo at POSTECH for supporting the photolithography process and photoemission analysis, respectively.

REFERENCES

(1) Rhee, S. W.; Yun, D. J. *J. Mater. Chem.* **2010**, *18*, 5437.

(2) Ma, H.; Yip, H. L.; Huang, F.; Jen, A. K. Y. *Adv. Funct. Mater.* **2010**, *20*, 1371.

(3) Murakami, T. N.; Gratzel, M. *Inorg. Chim. Acta* **2008**, *361*, 572.

(4) Steirer, K. X.; Berry, J. J.; Reese, M. O.; Hest, M. F. V.; Miedaner, A.; Liberatore, M. W.; Collins, R.; Ginley, D. S. *Thin Solid Films* **2009**, *517*, 2781.

(5) Geng, H. Z.; Kim, K. K.; So, K. P.; Lee, Y. S.; Chang, Y.; Lee, Y. H. *J. Am. Chem. Soc.* **2007**, *129*, 7758.

(6) Tantang, H.; Ong, J. Y.; Loh, C. L.; Dong, X.; Chen, P.; Chen, Y.; Hu, X.; Tan, L. P.; Li, L. J. *Carbon* **2009**, *47*, 1867.

(7) Geng, H. Z.; Kim, K. K.; Song, C.; Xuyen, N. T.; Kim, S. M.; Park, K. A.; Lee, D. S.; An, K. H.; Lee, Y. S.; Chang, Y.; Lee, Y. J.; Choi, J. Y.; Benayad, A.; Lee, Y. H. *J. Mater. Chem.* **2008**, *18*, 1261.

(8) Jackson, R. K.; Munro, A.; Nebesny, K.; Armstrong, N.; Graham, S. *ACS nano* **2010**, *4*, 1377.

(9) Hatton, R. A.; Blanchard, N.; Tan, L. W.; Latini, G.; Cacialli, F.; Silva, S. R. P. *Org. Electron.* **2009**, *10*, 388.

(10) Ou, E. C.; Hu, L.; Raymond, G. C. R.; Soo, O. K.; Pan, J.; Zheng, Z.; Park, Y; Hecht, D.; Irvin, G.; Drzaic, P.; Grunner, G. *ACS Nano* **2009**, *3*, 2258.

(11) Yu, W. J.; Kang, B. R.; Lee, I. H.; Min, Y. S.; Lee, Y. H. *Adv. Mater.* **2009**, *21*, 4821.
(12) Chang, C. H.; Chein, C. H.; Yang, J. Y. *Appl. Phys. Lett.* **2007**, *91*, 083502.
(13) Vaisman, L.; Marom, G.; Wagner, H. D. *Adv. Funct. Mater.* **2006**, *16*, 357.
(14) Kim, K. K.; Yoon, S. M.; Choi, J. Y.; Lee, J.; Kim, B. K.; Kim, J. M.; Lee, J. H.; Paik, U.; Park, M. H.; Yang, C. W.; An, K. H.; Chung, Y.; Lee, Y. H. *Adv. Funct. Mater.* **2007**, *17*, 1775.
(15) Ham, H. T.; Choi, Y. S.; Chung, I. J. *J. Colloid Interface Sci.* **2005**, *286*, 216.
(16) Datsyuk, V.; Kalyva, M.; Papagelis, K.; Parthenios, J.; Tasis, D.; Siokou, A.; Kallitsis, I.; Galiotis, C. *Carbon* **2008**, *46*, 833.
(17) Wu, T. M.; Lin, Y. W.; Liao, C. S. *Carbon* **2005**, *43*, 734.
(18) Chen, Y.; Kang, K. S.; Han, K. J.; Yoo, K. H.; Kim, J. *Synth. Met.* **2009**, *159*, 1701.
(19) Groenendaal, L.; Jonas, F.; Feitag, D.; Pielartzik, H.; Reynolds, J. R. *Adv. Mater.* **2000**, *12*, 482.
(20) Hwang, J.; Amy, F.; Kahn, A. *Org. Electron.* **2006**, *7*, 387.
(21) Jonsson, S. K. M.; Birgerson, J.; Crispin, X.; Greczynski, G.; Osikowicz, W.; Gon, A. W. D.; Salaneck, W. R.; Fahlman, M. *Synth. Met.* **2003**, *139*, 1.
(22) Yun, D, J.; Hong, K.; Kim, S. H.; Yun, W. M.; Jang, J.; Kwon, W. S.; Park, C. E.; Rhee, S. W. *ACS Appl. Mater. Interfaces* **2011**, *3*, 43.
(23) Najafi, E.; Kim, J. Y.; Han, S. H.; Shin, K. *Colloid Surf., A* **2006**, *284*, 373.
(24) Sham, M. L.; Kim, J. K. *Carbon* **2006**, *44*, 768.
(25) Chem., H.; Roy, A.; Back, J. B.; Zhu, L.; Dai, L. *Mater. Sci. Eng., R* **2010**, *70*, 63.
(26) Fan, B.; Mei, X.; Sun, K.; Ouyang, J. *Appl. Phys. Lett.* **2008**, *93*, 143103.
(27) Nguyem, T. P.; Rendu, P. L.; Long, P. D.; Vos, S. A. D. *Surf. Coat. Technol.* **2004**, *180*, 646.
(28) Chou, W. J.; Wang, C. C.; Chen, C. Y. *J. Inorg. Organomet. Polym. Mater.* **2009**, *19*, 234.
(29) Kwon, J. Y.; Kim, H. D. *J. Appl. Poym. Sci.* **2005**, *96*, 595.
(30) Yun, D. J.; Rhee, S. W. *J. Mater. Chem.* **2010**, *20*, 9754.
(31) Yun, D. J.; Lee, S. H.; Yong, K.; Rhee, S. W. *Appl. Phys. Lett.* **2010**, *97*, 073303.
(32) Jang, J. Y.; Nam, S.; Chung, D. S.; Kim, S. H.; Yun, W. M.; Park, C. E. *Adv. Funct. Mater.* **2010**, *20*, 2611.
(33) Smith, J.; Bashir, A.; Adamopoulos, G.; Anthony, J. E.; Bradley, D. D. C.; Hamilton, R.; Heeney, M.; McCulloch, I.; Anthopoulos, T. D. *Adv. Mater.* **2010**, *22*, 3598.